A Mechanically Powered 3500 mAh Mobile Phones Power-Bank

Sunday Adetona[1*], Michael Ige[1], and Raifu Salawu[2]
[1]Department of Electrical & Electronics Engineering, University of Lagos, Lagos, Nigeria;
[2]Department of Electrical & Electronics Engineering, The Bells University of Technology, Ota, Ogun State, Nigeria
*Corresponding author email: sadetona@unilag.edu.ng

Abstract
Research activities on implementation of mechanically powered phone chargers (MPPC) are receiving serious attention consequent upon the non-availability of power grids in many rural and remote areas of developing economies. These activities are further reinforced by the intermittent nature of the renewable energy resources for charging of mobile phones. The review of these already proposed MPPC revealed that most of them are not portable. Further, they have no facilities for controlling the charging and discharging of batteries. They are also not guided against direct charging of the batteries of mobile phones; thereby capable of damaging the batteries due to the poor quality of the energy they may produce. With these issues associated with the already proposed MPPC by various researchers, this study therefore proposes a reliable and portable mechanically powered 3500 mAh power-bank. The design is based on the Faraday's law of electromagnetic induction. The work addresses the issue of bulkiness by using a portable PD52103-12-4 ME planetary gear dc motor. The problem of excessive charging and discharging of the battery bank is solved by making use of LTC4056 and battery level visual indicators. In this proposed design, rather than charging the mobile phones directly, the power generated are stored in 3500 mAh power-bank before being used to charge the battery of a mobile phone. When tested, the proposed device charged a 3000 mAh Li-ion battery embedded in an android phone at rate of 0.37 percent per minute; and the various indicators glowed as expected.

Keywords: Battery bank; charger; mobile phone; planetary gear dc motor; and voltage regulator.

1.0 INTRODUCTION

Mobile GSM phones are not only used for the purpose of communication; they are also used for storing data, taking pictures, sending and receiving photos and files, and accessing the internet. And in the event of loss, some modern phones that are equipped with GPS App are employed to determine the location of a mobile phone or its user. Also, in the event of an emergency, with the help of a mobile phone, disaster can be averted, and lives can even be saved. These opportunities and many more are derivable from a good mobile phone if, and only if, it is available.

The availability of a good mobile phone is a function of the condition of the battery embedded in it. If the embedded battery is okay and reasonably charged, the phone would be available; and it would perform its various functions satisfactorily. However, if otherwise, it would not. The charging of the battery of a mobile phone is a regular activity that requires steady and quality electric power (Reddy *et al.*, 2013). The most efficient, common and economical way of obtaining electricity for the purpose of charging a mobile phone is through a power grid; which may not be available in many rural and remote areas of most developing economies (Matiur *et al.*, 2016). In fact, in many urban centres in these developing countries connected to the power grids, the electricity received from the grids are epileptic, and thereby making regular charging of the battery of the phone almost difficult and, sometimes, impossible. Charging of the phones while journeying is even a problem (Nikhil *et al.*, 2013; Kharudin *et al.*, 2016; and, Rocky *et al.*, 2017).

One way of solving this problem is by making use of renewable energy resources (Ayush and

Chinmay, 2011; Reddy *et al.,* 2013; Kharudin *et al.*, 2016; and, Atiqur *et al.*, 2016). The major issue that is associated with this method of charging battery of a mobile phone is, they are intermittent in nature (Kharudin *et al.*, 2016; and, Atiqur *et al.*, 2016). Besides, they are bulky and expensive. Researchers have tackled the problems of availability of electricity for charging a mobile phone anywhere and at any time of the day irrespective of environmental condition of the location, whether the power grid is available or otherwise; by proposing and implementing various types of mechanically powered phone chargers (MPPC). A typical example of the charger is the one proposed by Matiur *et al.* (2016), which is useful for charging batteries of phones in remote and isolated areas where there is no existence of power grid. It is also very useful in emergency situations, like natural disasters that may often lead to power failure. In a similar manner, in order to solve the problem of charging phones while journeying, Rocky *et al.* (2017) proposed a portable smart phone charger that uses human mechanical energy. In order to transform mechanical energy from a hand crank to a generator, a gear train and intermediate gears are used; therefore, it is quite bulky and less portable. Also, a mechanical hand crank mobile charger implemented by Nikhil *et al.* (2013) is another approach available for charging the mobile phones while journeying. In the device, a compound gear train and six intermediate gears are used for the energy transformation; thus, the device is less portable.

Instead of a single mechanically powered source charger proposed by many researchers, a hybrid mechanical charger that uses either hand crank or windmill mechanism at a time for charging of Nokia phones was proposed by Ayush and Chinmay (2011). The proposed device is achieved by using gear shifting mechanism, which makes the device bulky. In Reddy *et al.* (2013) and Kharudin *et al.* (2016), a mobile charger that makes use of either wind or geared dc generator or electrical power to charge a mobile phone that may not need be a Nokia phone, while journeying from one place to another place was proposed. Any one of the electric power sources can be selected to charge the mobile phone at a time. In Atiqur *et al.* (2016), a dual mode charger that makes use of hand circumvolve generator and photovoltaic was also proposed. The solar module is useful in daytime; while the hand circumvolve generator can be used at night. The design uses a compound gear train; hence, the proposed device is too big.

For the mobile phones’ and power banks’ batteries to last long, they should not be overcharged; and should not be fully discharged, at any time. To the best of our knowledge, most of the previous works on MPPC have no facilities for either preventing batteries excessive charge when being charged or safeguarding batteries from excessive discharge when being used. Secondly, most of them are not portable; as they cannot be carried easily from one place to another when journeying. Also, none of the previously proposed MPPCs focus on direct storage of the power generated in a high-power storage device for subsequent charging of mobile phones. This contribution therefore proposes a portable and reliable mechanically powered power-bank that will provide adequate electric power to charge mobile phones anywhere and at any time, irrespective of environmental conditions of the location, whether there is power grid or not.

The main goal of this study is achieved by designing a power bank charging device that does not need any external electrical power source; and by protecting the embedded battery bank in the device from damage that can occur as a result of overvoltage when the device is fully charged or over discharged. The issue of bulkiness is solved by using a 1:50 compound planetary gear dc motor; while the problems of excessive charging and dis-charging of the batteries are well addressed by introducing appropriate regulating circuits and battery level indicators to the proposed device. Also, energy generated by the proposed device is not supplied to the mobile phone directly; it is first stored in a 3500 mAh power bank and used for charging a mobile phone when the battery of the phone is drained.

2.0 RESEARCH METHODOLOGY

Figure 1 presents the schematic diagram of the proposed device. It consists of a generating unit, battery bank (BATT), battery charging unit, and battery level visual indicators.

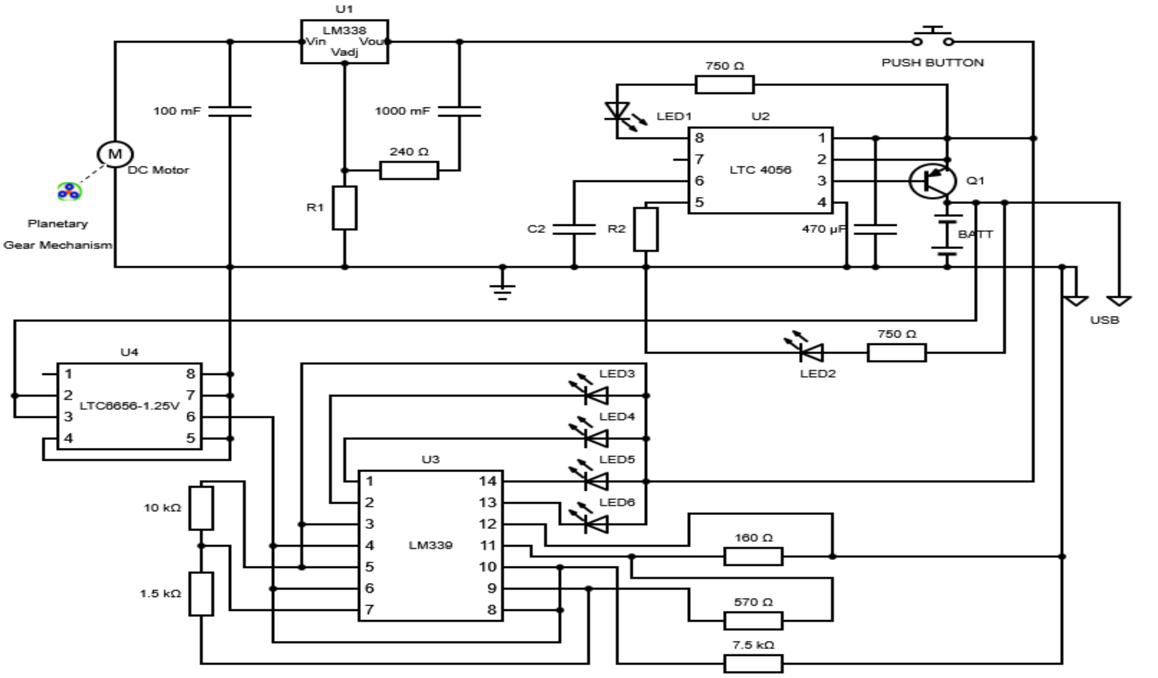

Figure 1. Schematic diagram of the proposed device

2.1 Selection of the embedded battery bank

In this work, Lithium Ion (Li-Ion) batteries are used. This is because they can be charged more quickly. Besides, they are used in places where a relatively great service life and thriftiness are necessitated (Matiur *et al.*, 2016). In Li-ion battery bank used, lithium cobalt oxide is a cathode, hard carbon is an anode, and gel polymer is an electrolyte (Lithium-ion Battery Team, 2009; and, Valoen and Shoesmith, 2007). During the discharging, lithium ions displace from the negative electrode to the positive electrode; and vice versa when charging.

The specification of the capacity rating (mAh) of the proposed MPPC is 3.7-5 V, 3500 mAh. This is because most Android phones' batteries rating capacities are about 3500 mAh. To achieve this, two pieces of 3.7-5 V, 18650 2200 mAh Li-Ion batteries are chosen and connected in parallel to form a bank. The manual of the selected battery is obtainable in TENERGY (Corporation, 2009). The charge/discharge efficiency ($\beth_{bat}$) of the selected battery has been found by Valoen and Shoesmith (2007) to be within 80–90 %; therefore, the effective capacity rating of the battery (mAh_{eff}) (Dorin *et al.*, 2013) is

$$mAh_{eff} = \beth_{bat} \times 2 \times mAh_{batt} \quad (1)$$

This gives $mAh_{eff} = 0.90 \times 2 \times 2200 \cong 3500mAh$

2.2 Design of Battery Charging Unit (BCU)

The BCU controls the charging of the embedded battery bank and protects them from overcharging and excessive discharging. This unit is built around a constant-current (constant-voltage) Li-Ion battery charger regulator; which is equipped with a programmable endpoint timer, LTC4056IC (U_2) (Linear Technology Corporation, 2003), and a 12V PNP low saturation switching transistor, ZXT1M322 (Q_1) (ZETEX, 2002). The Q_1 is used in this paper because it can withstand a nominal collector current of up to 4A (ZETEX, 2002).

In Figure 1, it is evident that the BATT is connected in between the collector terminal of Q_1 and ground. The resistor R_2 is used to programme the charging current (I_{CHG}). Whenever the BATT is at full charging, the collector current (I_{CQ1}) of Q_1 provides the I_{CHG}; whilst the emitter current (I_{EQ1}) of Q_1 flows through pin 2 of U_2, and through an internal current sense resistor (Linear Technology Corporation, 2003) embedded in U_2. The current (I_{Sense}) that flows out of the pin 2 of the U_2 has been established by Linear Technology Corporation (2003) to be

$$I_{Sense} = 915 \times I_{PROG} = 915 \times \frac{V}{R_2} \tag{2}$$

In Eq. 2, I_{PROG} is the current flowing out of the pin 5 of U_2; and knowing that,

$$I_{CQ1} = I_{CHG} = I_{BQ1} + I_{EQ1} = I_{BQ1} + I_{Sense} \tag{3}$$

Therefore, upon neglecting base current (I_{BQ1}) , Eq. 3 becomes

$$I_{CHG} = I_{Sense} = 915 \times \frac{V}{R_2} \tag{4}$$

According to Linear Technology Corporation (2003), V at pin 2 is 1 V; therefore,

$$R_2 = 915 \times \frac{1}{I_{CHG}} \tag{5}$$

This work is interested in rapid charging of the batteries embedded in the proposed device. The equation to obtain rapid charging current (TENERGY Corporation, 2009) is

$$I_{CHG} = 1C_A \tag{6}$$

where C_A is the nominal capacity of the battery bank to be charged (TENERGY Corporation, 2009). In this work $C_A = 3500\,mAh$; as such, $I_{CHG} = 3500\,mA$, therefore

$$R_2 = 915 \times \frac{1}{3500mA} \cong 270\,ohms \cong 0.27\,kohms$$

The charge round is terminated by a programmable timer; which is achieved by C_2 and R_2. In Linear Technology Corporation (2003), the total charge time is given as

$$Time\ (Hours) = 1.935 \times R_2 \times C_2 \tag{7}$$

The nominal charging time for charging of Li-Ion battery is about 1.5 hours (Lithium-ion Battery Team, 2009). In this work, we assumed that the rapid charging time would take 0.5 hours; therefore, to achieve this, C_2 should be

$C_2 = \frac{Time\ (Hours)}{1.935 \times R_2} = \frac{0.5}{1.935 \times 0.270} = 0.957\ \mu F \ \cong 1\ \mu F$

The charge round terminates when the time set by $R_2\ and\ C_2$ elapses; and the pin 8 of U_2 changes over from a firm pull-down to a feeble pull-down (Linear Technology Corporation, 2003). The charge round can be restarted by removing the input voltage and reapplying it; or if the voltage at pin 6 of U_2 falls below the recharge threshold, which is 4.05 V.

2.3 Battery Voltage Level Indicator

In the proposed device, a battery voltage level indicator that controls a bar graph meter that shows the status of the charge of a 3.7 V Li-Ion battery is shown in Figure 1. It consists of LM339 (U_3) (Texas Instruments Inc., 2018), an IC that contains four self-reliant voltage comparators that are to be operated from a single or dual power supplies over a wide range of voltages and a precision low drift low noise buffered reference, 1.25V LTC6652-1.25 (U_4) (Brendan, 2009, and Linear Technology Corporation, 2007). The U_3 has an open collector output that drives 15 mA, low power consumption (Texas Instruments Inc., 2018).

In the battery voltage level indicator, all the non-inverting inputs of the comparators embedded in U_3 are connected to the output pin of U_4; whereas, their inverting inputs are connected to consecutive points on a voltage divider. The LEDs illuminate as the voltage at the inverting terminals exceeds the reference voltage that is set by U_4. The LED_6, LED_5, LED_4 and LED_3 turn on at 1.60 V, 1.63 V, 1.75 V, and 2.07 V respectively.

2.4 Generating Unit

The generating unit of the proposed device consists of the planetary gear dc motor (M) and voltage regulator (U_1).

2.4.1 Selection of the planetary gear dc motor

In this work, the dynamo is the main source of electrical power in charging battery bank in order to have the needed backup. The dynamo converts mechanical rotation into a pulsing dc. Its operation is based on Faraday's law of electromagnetic induction.

The electrical power (P_e) (Ayush and Chinmay, 2011; and, Rocky *et al.*, 2017) required to charge the Li-Ion battery bank in the proposed device is

$$P_e = I_{CHG} \times V_t \tag{8}$$

where, $V_t = battery\ voltage = 4.2\ V, and\ I_{CHG} = 3500\ mA$, therefore, P_e is 14.7 W.

From the law of conservation of energy, the mechanical power (P_m) (Ayush and Chinmay, 2011) required to drive the dc motor to generate the required P_e is given by

$$P_m = P_e + P_l \tag{9}$$

In Eq. 9, P_l is power losses; and it is assumed to be $50\,\%\ of\ P_e$; therefore, $P_m = 1.5\,P_e$. The expected P_m when the dc motor is cranked would therefore be 22 W at 12 V.

Most of the dc motors that generate 22 W at 12 V require nominal rotational speeds of 3100 rpm to be applied to their shafts; whereas, when hand cranking, the rotational speed that can be applied to the shaft will be low. As a result, the generator will produce a low voltage. Torque and rotational speed can be increased or decreased in the ratio of the number of teeth (Kwon and Kahraman, 2015) in the driving and driven gears.

To gear up the rpm of the generator to generate greater electrical power at specified voltage, in this paper, a planetary gear train that is already incorporated with a dc motor is used. This is because the planetary gear train is more compact. The tightness is made possible because epicyclic gear sets use evenly separated planets, and this ensures least possible radial bearing reinforcement requirements (Ligata et al., 2007). Epicyclic gear sets also attain higher power density level than the fixed–center parallel-axis gear trains (Kwon and Kahraman, 2015; Ligata *et al*., 2007). Has shown in Figure 2, the various components of the epicyclic gear are Sun (S), Planets (P), Planet Carrier (C), and Ring (R) (Galvagno, 2010).

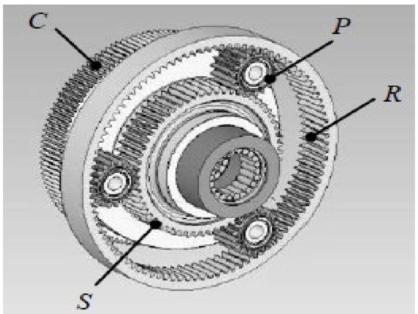

Figure 2. Planetary gear System

In the gear mechanism used in this paper, the ring gear is held stationary, the input rotation (ω_S) is rendered by the sun gear, and the planetary gear carrier created the output rotation (ω_C). It has been revealed in Litvin and Fuentes (2004) that the gear ratio of the planetary gear mechanism is,

$$\gamma = \frac{\omega_S}{\omega_C} = \frac{Angular\ velocity\ of\ the\ sun\ gear}{Angular\ velocity\ of\ the\ carrier\ gear}$$

$$\gamma = 1 + \frac{r_R}{r_S} = 1 + \frac{N_R}{N_S} \quad (10)$$

where, N_R and N_S are numbers of teeth in ring and sun gears respectively; whereas, r_R is the radius of ring gear, and r_S is the radius of the sun gears of the planetary gear system. This equation shows that if N_R, N_S, r_R and r_S are known, the gear ratio can be determined; but in this study, the known parameters are rotational speeds on sun and carrier gears.

In Eq. 10, $\omega_S = \frac{2\pi n_S}{60}\ and\ \omega_C = \frac{2\pi n_C}{60}$; where, n_s and n_C are rotational speeds on sun and carrier gears respectively. If it is assumed that 60 rpm is applied to the hand crank of the proposed device, which is n_s the expected n_C from the carrier of the planetary gear mechanism that would be transmitted to the shaft of the dc motor, is 3100 rpm. For the gear system to be effective, its gear ratio must therefore be,

$$\gamma = \frac{n_S}{n_C} = \frac{60}{3100} = \frac{1}{52} \cong \frac{1}{50}$$

This shows that for one full rotation of the hand crank attached to the dynamo through a planetary gear mechanism, the rpm that would be available to work on the dc motor is approximately *50 x hand crank rpm*. With this information, a portable PD52103-12-4 ME planetary gear dc motors (Transmotec Inc., 2018), is therefore selected as the main generator. The orthogarphic view of the motor is shown in Figure 3.

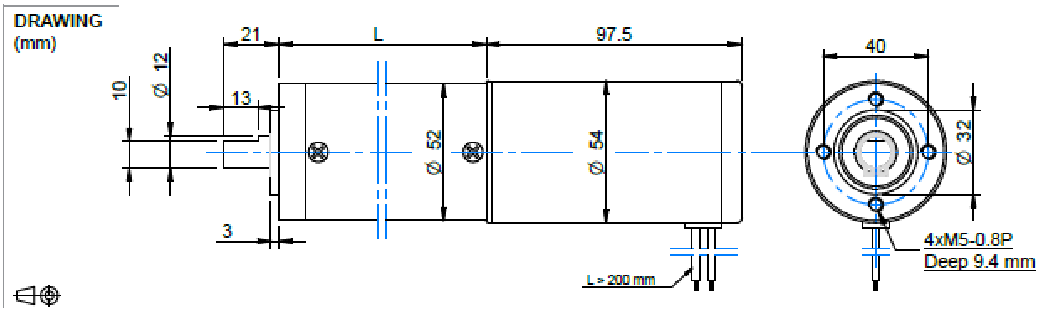

Figure 3. Orthographic view of the planetary gear dc motor

2.4.2 Voltage Regulator

The output voltage from the planetary gear dc motor ranges from 5 V to12 V; whereas, the Li-Ion battery bank to be charged requires voltage ranging from 3 V to 4.22 V. This is because the full charge state will provide $4.2\,V \pm 0.02\,V$ on the battery bank, whereas the float charge will provide 3.0 V. At the beginning of the charge round, the charger draws a 3.5 A; though, the current falls gradually as the charging continues to a current limit of 22 mA. With this information, LM338 (U_1), an adjustable 3-terminal positive voltage regulator (SGS-Thomson Microelectronics, 1994), is selected and utilized. The IC is capable of handling about 5 A current over a 1.2 V to 32 V output range.

The output voltage V_0 of the U_1 has been established by SGS-Thomson Microelectronics (1994) to be

$$V_0 = 1.25V\left(1 + \frac{R_1}{R_0}\right) \tag{11}$$

where, $R_0 = 240\ ohms$(SGS-Thomson Microelectronics, 1994); as such, to obtain an output voltage of 5 V, when 12 V is applied at input port of U_1, $R_1 \cong 750\ ohms.$

2.5 Mode of Operation

The schematic diagram of the proposed device is shown in Figure 1. When the hand crank is turned anticlockwise, the speed(rpm) produced by the hand is stepped up by the planetary gear mechanism embedded in the dc motor; and this produces a dc voltage (5-12 V) by the dynamo, which is regulated by U_1. The regulated dc voltage obtained is then fed into U_2; which in turn is also connected to Li-Ion battery bank for proper charging and power cutoff from the battery when full. The U_2 has two indicators, the LED_1 (Red LED) which indicates charging; while the LED_2 (Green LED) shows that the battery bank is full. The U_3 ensures proper battery level indication; and it consists of four operational amplifiers.

The charging cycle starts when the voltage obtained from the generating unit of the proposed device is greater than or equal 4.4 V, at that point the voltage across R_2 will be greater than

0.82 V; which is shutdown threshold voltage. At the kick-off of the charging round, if the voltage across the BATT is less than 2.8 V, U_2 trickles charge the BATT. This is done in order to bring the voltage across BATT up to a secured level for the commencement of charging at full current. In this mode, pin 6 of U_2 receives an approximately 2 % of the programmed charge current from internal current source. Immediately, the voltage at the pin 6 of U_2 is more than 2.9 V, U_2 enters the full charge constant current mode. In this mode, the charge current is I_{CQ1}; and as the battery bank charges, its voltage rises. Whenever the battery bank voltage attempts to surpass 4.2 V, an internal amplifier in U_2 will turn away current from the output driver; thereby fixing charging current to sustain 4.2 V on the BATT. When the charge time set by R_2 and C_2 lapses, the charging round stops; and pin 8 of U_2 transits from a firm pull-down to a feeble pull-down. The charging round can be restarted by simply switching on and off a momentary button. When the input power is removed, the leakage currents from the BATT bank will be drained by U_2; as such, the BATT stick by time will be maximized.

The output voltage from the battery bank is connected to a USB hub for transfer of power to the mobile phone. The whole device can be switched on and off by a momentary button; which is also used in activating the LEDs and USB charging hub. This study also makes provision for electrical source of charging phones where electricity is available to avoid the stress involved in cranking the device.

3.0 RESULTS

3.1 Preparation for charging

The proposed device is cranked with the aid of the hand crank, Figure 4, to charge the battery in it. Figures 5 and 6 show photographic views of the interior and exterior sections of the proposed device. It is switched on by pressing the red power button in Figure 6. This action prepares the proposed device for a charging or discharging activity.

Figure 4. Hand Crank

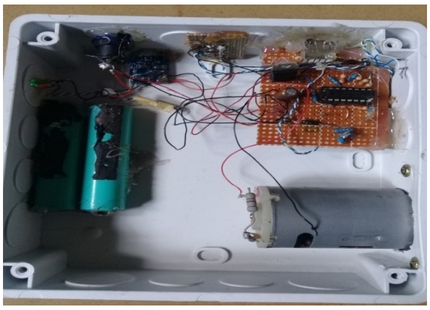

Figure 5. Proposed device interior connections

3.2 Experimental Set Up and Results

Figures 7 through 9 show the setup of the proposed device with(without) an Android mobile phone. When the proposed device is not fully charged the four red LED light indicators glow at various voltage levels. Figure 7 indicates that the three out of the four LEDs are glowing, and this indicates that the device is 75 % charged. In Figure 8, a mobile phone is not connected to the device. During cranking, the red light under the green LED comes up, Figure 9. This stays on until the device is fully charged when the green LED glows. When the device is fully charged the red LED goes off remaining only the green LED glowing. Thus, the device can be used for charging battery of a mobile phone. As such, an android phone which its battery usage level indicated 28 % was connected to it. Figure 9 depicts the mobile phone under charging.

Figure 6. Proposed device casing with connection ports

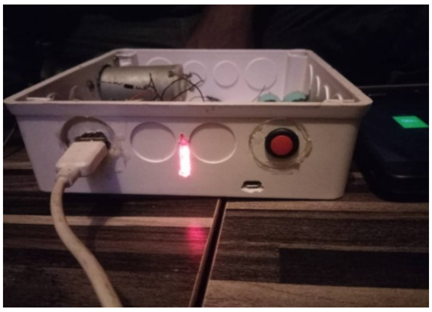

Figure 7. Photographic view proposed device not fully charged with mobile phone

Figure 8. The photographic view of the fully charged proposed device without mobile phone connected while cranking with the power button ON.

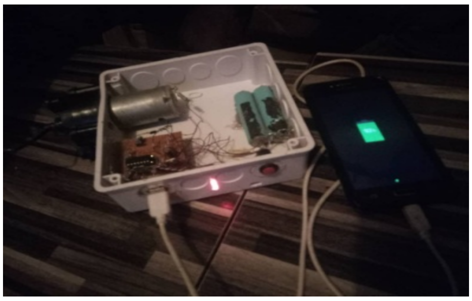

Figure 9. The photographic view of the fully charged proposed device with mobile phone connected and being charge

4.0 DISCUSSION

The proposed device was cranked for 45 minutes, and on measuring the voltage at its USB hub port when fully charged, the maximum output voltage obtained at the port was 4.96 V; whereas, the input dc voltage to the voltage regulator circuit was recorded to be 12 V. This shows that LM338 has regulated the dc voltage to 4.96 V. The maximum output voltage of the fully charged device is therefore 4.96 V.

An android phone that has an inbuilt 3000 mAh battery was connected to the fully charged proposed device. The battery usage of the android phone before connection was found to be 28 %. The percent charge of the battery of the phone by the proposed device was taken at an interval of 10 minutes. The result obtained is presented in Figure 10. The plot reveals the rate of charging of an android phone against time (minutes) using the proposed device is about 0.37 percent per minute.

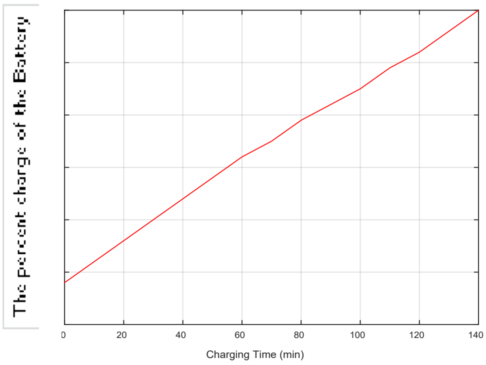

Figure 10. The plot of % charge versus Time

The total cost of production of the proposed device is about ₦10, 000.00, but it will cost less if it is manufactured in large quantities

5.0 CONCLUSIONS

This study reviewed research activities on the design and implementation of MPPC. It established that most existing designs are not portable and that equally lack facilities for controlling the charging and discharging of the batteries. Further, these existing designs directly charge the batteries of the mobile phones; hence the batteries may be damaged due to the poor quality of the energy they may produce. The issues associated with the already proposed MPPC by various researchers are addressed in this paper.

This study addresses the issue of bulkiness by using a portable PD52103-12-4 ME planetary gear dc motor, the problem of excessive charging and discharging of the battery bank is solved by making use of LTC4056 and battery level visual indicators; and instead of charging the mobile phones directly, in this paper, the power generated are stored in 3500 mAh power bank before using it to charge the battery of a mobile phone.

When tested, the proposed device charged a 28 % discharged 3000 mAh Li-ion phone at rate of 0.37 percent per minute; and the various indicators glowed as expected. The proposed device can be improved upon by increasing the rating capacity of the power bank by increasing the total number of batteries in the bank appropriately and introducing and adjusting necessary components that would support the additional rating capacity.

ACKNOWLEDGEMENT

The authors are pleased to acknowledge the support provided by the Department of Electrical and Electronics Engineering (DEEE), University of Lagos, Lagos, Nigeria.

REFERENCES

Reddy N.R.R., Sreekanth Y., and Narayana M., (2013). Mechanical and Electrical Mobile Charger. *International Journal of Engineering Research and Applications*, 3**(6)**: 1705-1708

Matiur R., Mamun A., and Rabbi M.F., (2016). Design and Implementation of Mechanically Powered Battery Charger. *ARPN Journal of Engineering and Applied Sciences*, 11**(3)**: 1914-1917.

Nikhil K.J., Aravind V., Eranki V.S., Krishna P., Chakravarthy K.Y., (2013). Virtual Prototype of Mechanical Hand Crank Mobile Charger. *International Journal of Innovative Technology and Exploring Engineering (IJITEE)*, 2(**2):** 52-54.

Kharudin A., Wan S.W.M., Damhuji R., Muaz I.A., Asyraf M., and Tg A.A., (2016). Design and Implementation of Portable Mobile Phone Charger using Multi Directional Wind Turbine Extract. *Indian Journal of Science and Technology*, 9**(9)**: 1-6.

Ayush R.J., and Chinmay V.H., (2011). Hybrid Mechanical Charger. *International Journal of Scientific and Engineering Research*, 2**(5)**: 1-3.

Atiqur R., Nusrat H., Nipu K.D., Furial N.M., and Morshed A., (2016). Portable Dual Mode Mobile Charger with Hand Crank Generator and Solar Panel. *Indonesian Journal of Electrical Engineering and Computer Science*, 1**(2):** 282-287.

Rocky C., Thanarat C., Khandakar A., Anit C., and Sajid H., (2017). Portable Smart Phone Charger using Human Mechanical Energy by Gear Train with Hand Crank. *IOSR Journal of Electrical and Electronics Engineering (IOSR-IEEE)*, 12**(3)**: 20-25.

Lithium-ion Battery Team, (2009). Lithium Ion Rechargeable Batteries. *Technical Handbook* https://web.archive.org/web/20090411024100if_/http://www.sony.com.cn:80/products/ed/battery/download.pdf, Accessed 29/07/ 18

Valoen, L.O., and Shoesmith, M.I., (2007). The effect of PHEV and HEV duty cycles on battery and battery pack performance*. Proceedings of 2007 Plug-in Highway Electric Vehicle Conference*.

http://umanitoba.ca/outreach/conferences/phev2007/PHEV2007/proceedings/PluginHwy_PHEV2007_PaperReviewed_Valoen.pdf, Accessed 23 /04/18.

Dorin S., Dan P.D., and Tirnovan R., (2013). Method for Determining the Effective Capacity Variation Depending on the Discharge Current for Lead-Acid Calcium Batteries, *Proceedings of the 8th International Symposium On Advanced Topics In Electrical Engineering*, May 23-25, 2013, 1-7.

TENERGY Corporation, (2009). TENERGY 18650 2200mAh Li-Ion Cell, Tenergy Corporation. http://www.allbattery.com/productimages/liion/Data%20sheet%2018650%202200mAh.pdf, Accessed 23/04/18.

Linear Technology Corporation, (2003). LTC4056-4.2, Linear Li-Ion Charger with Termination in ThinSOT, Analog Devices, Inc. https://www.analog.com/media/en/technical-documentation/data-sheets/405642f.pdf, Accessed 23/11/18.

ZETEX, (2002). MPPS™ Miniature Package Power Solutions: 12V ZXT1M322 PNP Low Saturation Switching Transistor. https://www.diodes.com/assets/Datasheets/ZXT1M322.pdf, Accessed 23/11/18.

Texas Instruments Inc. (2018). LM339, LM239, LM139, LM2901 Quad Differential Comparators datasheet (Rev. U), http://www.ti.com/lit/ds/symlink/lm339a.pdf, Accessed 23/11/18..

Brendan W., (2009). How to Choose a Voltage Reference. *Linear Technology Magazine*, 19**(1)**: 14-19.

Linear Technology Corporation, (2007). LTC6652: Precision Low Drift Low Noise Buffered Reference, https://www.analog.com/media/en/technical-documentation/data-sheets/6652fg.pdf, Accessed 29/07/18.

Kwon H.S., and Kahraman, A.A., (2015). Influence of Design Parameters on Mechanical Power Losses of Planetary Gear Sets. *Proceedings of the ASME International Design Engineering Technical Conferences and Computers and Information in Engineering Conference*, August 2-5, 2015, 1-8.

Ligata H., Kahraman A., and Singh A., (2007). An experimental investigation of the influence of manufacturing errors on the planetary gear stresses and load sharing, *Proceedings of the ASME International Design Engineering Technical Conferences and Computers and Information in Engineering Conference,* Sep. 2007, 149-158.

Galvagno E., (2010). Epicyclic gear train dynamics including mesh efficiency. *International Journal of Mechanics and Control*, 11**(2):** 41-47.

Litvin F.L., and Fuentes A., (2004). Gear Geometry and Applied Theory, 2nd edition, Cambridge University Press, New York, 2004, 697-699.

Transmotec Inc., (2018). Ø 43 - 123 mm, 12 -421W: Planetary gear dc motors. https://www.transmotec.se/wp-content/uploads/2018/10/Transmotec-EN-PD-12W-450W-2018-3.pdf, Accessed 29/07/18.

SGS-Thomson Microelectronics, (1994). LM138/238/338, Three-Terminal 5-A Adjustable Voltage Regulators, http://pdf.datasheetcatalog.com/datasheet/SGSThomsonMicroelectronics/mXurqzq.pdf, Accessed 29/07/18.